State of Health Analysis for Large-Scale Lithium-Ion Batteries based on Gaussian Process Regression Machine Learning

Grant M. Fischer, Rishab Nanduri, and Dan M. Ionel

SPARK Laboratory, Stanley and Karen Pigman College of Engineering, University of Kentucky, Lexington, KY, USA
grant.fischer@uky.edu, rishabn029@gmail.com, dan.ionel@ieee.org

***Abstract*—Deployment of large-scale lithium-ion (Li-ion) battery energy storage systems (BESSs) in modern grid operations is growing. As utilization expands, aging becomes a critical factor affecting long-term performance, reliability, and economic viability. Characterization of battery degradation based on long-term field data remains limited. In this paper, an example dataset containing six years of high-resolution data from a field deployed 1MW/2MWh Li-ion BESS is analyzed. An algorithm based on Gaussian process regression (GPR) machine learning is developed to estimate and predict the state of health (SoH) of large-scale BESSs. The algorithm trains utilizing several system-level input features, including battery management system (BMS) reported SoH, for three applied methods: estimation, static prediction, and adaptive prediction. The adaptive prediction method is designed to continuously refit on an expanding dataset, and the estimation method uses five fold cross validation to test its ability to fill in gaps of data. The estimation model yields a percent MAE of 0.192 and RMSE of 0.640. Excluding an event following an extended outage, the adaptive refitting prediction model yields percent MAE and RMSE of 0.120 and 0.163 respectively. The evolution of the example battery's reported SoH is studied to review experimental challenges for BESS analysis.**

***Index Terms*—State of Health, Gaussian Process Regression, Machine Learning, Battery Energy Storage System, Calendar Aging, Cycle Aging.**

I. Introduction

Lithium-ion (Li-ion) batteries play an important role in the future resilience, stability, and reliability of the power grid, and they offer the flexibility to support balancing services and peak load management [1]. These energy storage applications could be utilized to support new grid integrations such as distributed energy resources and large loads, including data centers. Some factors that restrict the application and deployment of Li-ion batteries are limited accuracy of projected lifetime estimates and limited cycle life caused by electrochemical, mechanical, temperature related, and operationally inflicted aging factors [1], [2]. Tracking the rate of this aging is an important area of energy storage research given how improving the lifetime could benefit grid applications. Developing methods to accurately estimate and predict the battery aging is difficult due to the various linear and nonlinear degradation patterns that Li-ion batteries can experience over the course of their lifetime and the limited availability of real field data needed to study these behaviors [3].

To account for the complex factors influencing degradation, adaptive machine learning models can be designed to train on all previous events before making each prediction, incrementally expanding the training set as new measurements become available [4], [5]. In addition to nonlinear aging, field operating conditions and limited diagnostic data can increase uncertainty in state of health (SoH) estimation, further increasing the difficulty of developing accurate models [6]. These sources of uncertainty could pose a further challenge for developing aging prediction and estimation models for large-scale battery energy storage systems (BESS), which can have naturally inconsistent operating profiles and extended idle periods. One approach to counter these limitations includes Gaussian processes, a flexible modeling method suited for limited data that has been applied for battery field data with uncontrolled operating conditions [7].

This paper utilizes six years of operational data from an example large-scale 1MW/2MWh Li-ion BESS dataset, including high-resolution power, SoC, and voltage data. An analysis of the SoH during this period is performed, including cycle and calendar related aging factors. A Gaussian process regression (GPR) machine learning algorithm, including SoH estimation and adaptive prediction methods proposed for large-scale BESS applications, is developed and tested. The estimation method is proposed for filling gaps in past data, and the adaptive prediction method is proposed for future SoH projection. The algorithm considers the SoH data in the example dataset and incorporates several input features including average cell voltage and charge and discharge energy. While GPR methods have been applied for cell level and smaller scale battery applications, this algorithm is proposed and applied for large-scale BESS datasets.

II. Long-term Field Data with an Example from Utility-Scale BESS Field Pilot

The example data employed to illustrate the proposed GPR algorithm is provided by the publicly available large-scale 1MW/2MWh field pilot BESS dataset from the battery installed and operated on the PPL Renewable Integration Research Facility, as previously reported in [8], [9]. This battery contains 20 racks, each with 17 LG ChemM48126P3B1 battery modules rated for 126Ah at 51.8V nominal voltage [10].

Authors' manuscript version accepted for publication. The final published version will be copyrighted by IEEE and will be available as: Fischer, G. M., Nanduri, R., and Ionel, D. M., "State of Health Analysis for Large-Scale Lithium-Ion Batteries based on Gaussian Process Regression Machine Learning," Proceedings, IEEE International Conference on Renewable Energy Research Applications (ICRERA), Paris, France, 5p (October 2026). ©2026 IEEE Copyright Notice. "Personal use of this material is permitted. Permission from IEEE must be obtained for all other uses, in any current or future media, including reprinting/republishing this material for advertising or promotional purposes, creating new collective works, for resale or redistribution to servers or lists, or reuse of any copyrighted component of this work in other works."

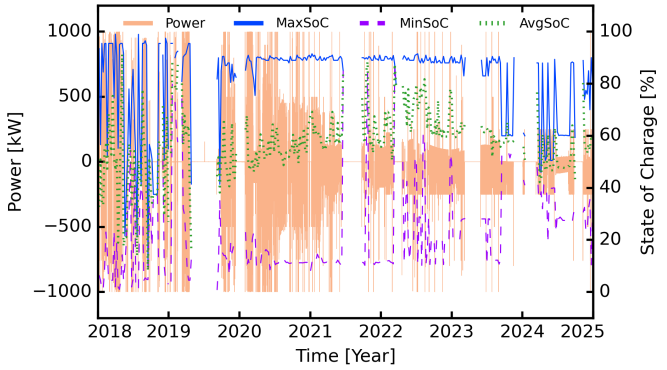

Fig. 1. Variation of system power and SoC from 2018 through 2024, highlighting high power draw in the early years and reduced operation after 2023. This is characterized by initial deep SoC cycling, with high maximum and low minimum recorded values, followed by a narrower operating range.

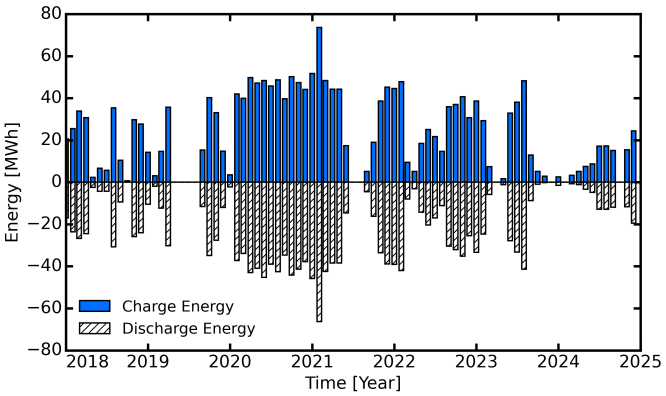

Fig. 2. Total monthly charging and discharging energy over the studied time frame. The highest cumulative bi-directional energy throughput is recorded between 2020 and 2022.

This unit has operated continuously since its commissioning in 2017, supporting various experimental research efforts over the course of its lifetime, and has provided a publicly available long-term high-resolution operational dataset that is utilized in this study.

The operational power and state of charge (SoC) data from 2018 through 2024 is plotted in Fig. 1. It can be observed that the maximum and minimum weekly SoC and the power draw magnitude are reduced over time. Starting towards the end of 2023, the number of times the battery is used at rated power or to the SoC limits is reduced due to new operational procedures as a safety precaution, as explained in [8]. The cumulative bi-directional energy throughput is charted in Fig. 2 with the monthly charge and discharge energy, showing the highest throughput between 2020 and 2022 before declining to its lowest in 2024.

The operating conditions of the system can impact battery aging. As a metric used to quantify aging, SoH can represent the percentage capacity-based change of the battery when at full charge relative to its start of life maximum capacity, or it can represent the increase of internal resistance over time [11]. The battery management system (BMS) for the BESS and dataset analyzed in this paper computes the SoH percentage to represent the system level aging. A 2016 paper

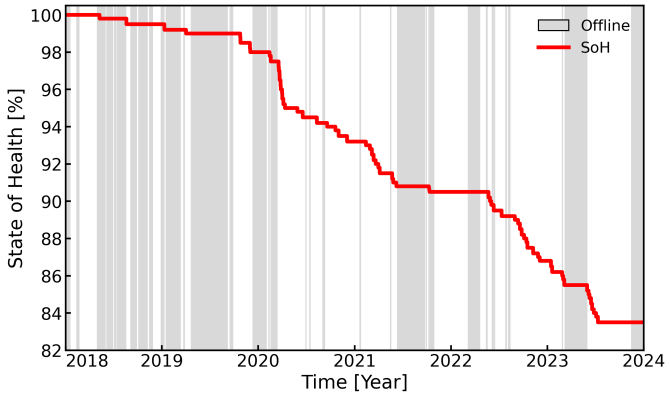

Fig. 3. Evolution of the nonlinear battery aging over the studied time frame in reported changes to SoH percentages. In the periods when the BESS was offline, SoH updates reported by the BMS were limited.

by Berecibar *et al.* reviewed BMS experimental techniques for estimating battery SoH, which were summarized to operate by storing cycling data history and evaluating against the main parameters affecting the battery lifetime [12].

The SoH analysis focuses on the period from 2018 through 2023, when the battery operated at its rated power over a wider SoC range, providing more frequent BMS reported SoH updates and enabling a more comprehensive characterization of battery aging before the operational changes introduced in late 2023. This SoH data is plotted in Fig. 3 and shows a net reduction from 100% in 2018 to 83.5% in 2023. The aging of the battery is nonlinear, and will be analyzed in greater detail in Section III. The SoH plot highlights offline periods that last more than a day when the operational BESS undergoes planned and unplanned outages [8]. The reported updates for SoH by the BMS during these periods are limited.

III. Large-scale BESS Aging Analysis incl. Calendar and Cycle Based Aging Factors

To determine input features for the development of the GPR algorithm for large-scale BESSs, the example BESS dataset is analyzed considering annual operating statistics, calendar aging, and cycling aging. The SoH incremental reduction and relevant annual statistics are included in Table I. Bi-directional energy throughput and full equivalent cycles (FECs) are used to represent the annual cycling of the BESS. The FECs can be calculated using the equation

$$\mathrm{FEC} \approx \frac{0.5 \int |P_{\mathrm{batt}}(t)|\, \mathrm{d}t}{E_{\mathrm{batt}}^{\mathrm{nom}}}, \tag{1}$$

where $P_{\mathrm{batt}}(t)$ is the battery power draw and $E_{\mathrm{batt}}^{\mathrm{nom}}$ is the nominal energy battery capacity [13]. The average non-zero power shows that the battery is operated at higher power draw in the initial years, as also seen in Fig. 1. The proportionally larger offline percentage in the first two years results in those periods having lower average power and less cycling.

A study by Lam *et al.* stored various Li-ion cells, including NCR and LFP cell types, for up to 13 years to analyze cell-level calendar aging at static SoC and temperature conditions [14], [15]. This calendar aging reference data is included in

Table I
ANNUAL BESS OPERATING STATISTICS AND INCREMENTAL SOH REDUCTION.

Year	SoH End	Incremental SoH Reduction [%]	Bi-directional Throughput [MWh]	FEC	Avg. Power [kW]	Avg. Non-zero Power [kW]	Offline [%]
2018	99.5	0.5	422.1	105	48.2	185.2	45.6
2019	98.0	1.5	312.1	78	35.6	152.5	61.4
2020	93.2	4.8	948.7	237	108.0	180.7	10.3
2021	90.5	2.7	726.6	181	83.0	189.1	34.5
2022	86.8	3.7	609.3	152	69.6	133.3	16.2
2023	83.5	3.3	394.4	98	45.0	100.8	36.0

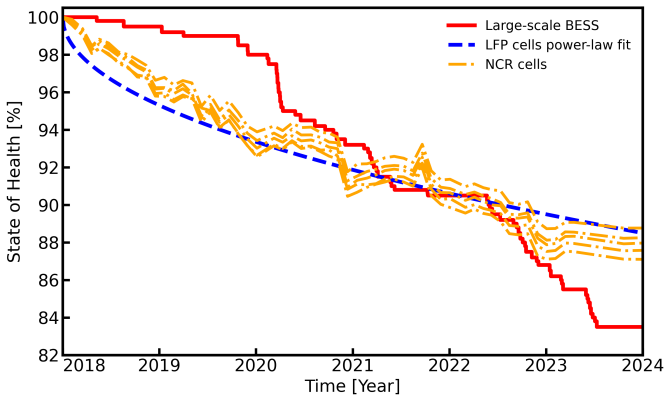

Fig. 4. Example large-scale BESS SoH overlaid with the referenced calendar aging SoH data from the public dataset in [14], [15]. These profiles include Li-ion NCR cell aging data and a curve fit to LFP cell data, estimated using the power law in equation (2).

Fig. 4, overlaying six years of storage data from NCR and LFP cell-level data with the system-level BESS SoH. The LFP SoH curve is calculated using the power law in equation (2)

$$\mathrm{SoH}(t) = 100 - \alpha \cdot t^{\beta}, \tag{2}$$

where t is time measured in weeks, α accounts for the pre-exponential rate of degradation, and β accounts for the time-dependent degradation. The curve is estimated to match the referenced incremental power law end of life extrapolation curve data for LFP cells [14].

During these initial years with higher offline percentages and less cycling, the reported example BMS SoH data shows that the BESS dataset ages more slowly than the reference cell-level NCR and LFP calendar aging curves. The BESS storage conditions, design, and cell chemistry are all factors that could alter the relative contribution of calendar aging to SoH reduction [16]. The BESS experienced a 2% BMS reported SoH reduction over the first two years, and the years with comparatively higher bi-directional energy throughput were associated with more SoH reduction on average. The only year with more than 200 FECs was 2020, which had the largest incremental reported SoH reduction at 4.8%. This analysis motivates the focus on cycling related aging and the inclusion of charge and discharge energy as first input features in the development of the GPR algorithm.

IV. GAUSSIAN PROCESS REGRESSION FOR AGING ESTIMATION AND PREDICTION

While GPR has been recently applied for other smaller battery systems [17], the GPR algorithm in this paper is developed to be applied for large-scale field BESS with operational datasets. This section details the development and data preparation for the GPR machine learning algorithm for large-scale BESS aging estimation and prediction. The BESS data represents an example for the analysis and application of this algorithm to large-scale BMS reported SoH data with operational profiles. The proposed framework for the GPR adaptive model is shown in the flowchart in Fig. 5. There are three applied methods using the GPR algorithm: SoH estimation using shuffled five fold cross validation, static prediction as a base prediction case, and adaptive prediction with continuous refitting. The estimation method is developed to fill past gaps in large-scale BESS SoH datasets, and the adaptive prediction method is developed to project future SoH values. For these tests, the analyzed dataset spans 2018-2021.

The algorithm developed for the estimation and the associated prediction methods are based on the SoH values reported by the manufacturer proprietary BESS BMS. Manufacturer and owner firmware and software updates, such as one that occurs in the example BESS in 2019 [8], may impact the consistency of the SoH values reported by the BMS. Additionally, ambient conditions not observed by the developed model, such as weather, may influence the BESS operation including the SoH [8].

Because of the relevance of the energy data to SoH changes as established in Section III, the energy charge and energy discharge metrics were included as important input features in the GPR algorithm. As the model was improved, average cell voltage was also included as an additional input feature. Input sensitivity testing was performed by tracking the output SoH error when each input feature was shuffled. Apart from the previously reported BMS SoH values, the charge and discharge energy features were found to have the greatest impact on SoH accuracy, exceeding cumulative time, time elapsed since the previous training event, and cell voltage features.

The data for the algorithm is prepared for each case by searching for deep SoC cycles, defined as GPR training events, where a full sweep from less than 12% to greater than 88% SoC is detected, and then the input feature data was extracted and cleaned. This search captures similar cycle data points

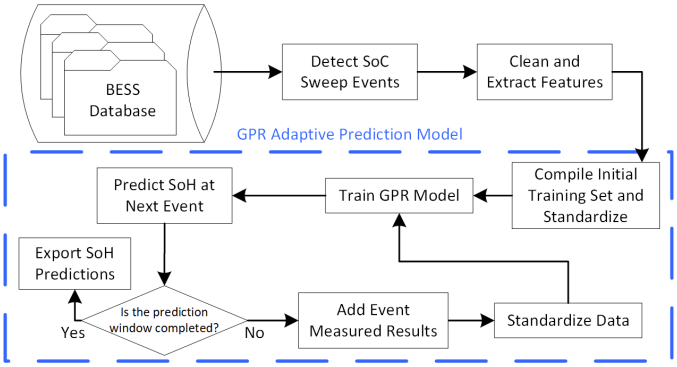

Fig. 5. Adaptive GPR model including SoC sweep detection and data preparation. The adaptive model incrementally adds BESS measured SoH events for the model to be refit for each new SoH prediction.

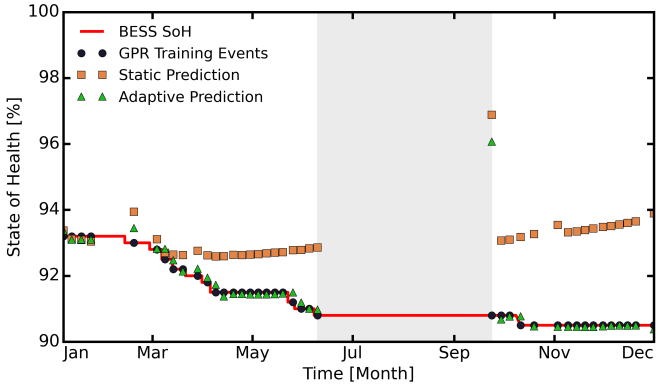

Fig. 6. Static and adaptive GPR prediction results plotted with the BESS's reported operational SoH values. The adaptive method sees considerable improvement over the static prediction method and accurately predicts the majority of training events.

with near full coverage of the battery's maximum capacity to train the GPR algorithm, allowing the machine learning model to capture changes in the feature inputs on consistent profiles in the operational dataset.

An adaptive prediction method is fit using the 2018 through 2020 GPR training events and then predicts the SoH value for the first event in 2021. For each new prediction, the model is refit for all past reported input features in the dataset, including the data from the most recent training event. A static prediction method, without continuous refitting, is tested to show the advantage of adaptively refitting the GPR model to maintain the most accurate results. The SoH GPR predictions are plotted in Fig. 6, where the static prediction method initially accurately predicts the reported experimental values before failing to follow the changing trends due to nonlinear aging of the BESS. By comparison, the adaptive method performs substantially better, maintaining accurate predictions for nearly all GPR training events.

The estimation method performs a shuffled five fold cross validation of the training events, estimating the SoH value of all data points after five rounds of model prediction, each round withholding a different fifth of the dataset. The validated method can be utilized to estimate SoH values in the gaps of SoH data for large-scale BESSs. The offline period in Fig. 6 highlighted in gray contributes to a prediction outlier on September 23rd when the battery comes back online after an over three month long gap. This operational gap limits the performance of the developed model during extended outage periods, which calendar aging projections and temperature input feature data may help address in future development. The GPR estimation method could be utilized to support efforts to fill these gaps if experimental SoH training data is obtained during offline periods when changes in SoH are not reported by the BMS.

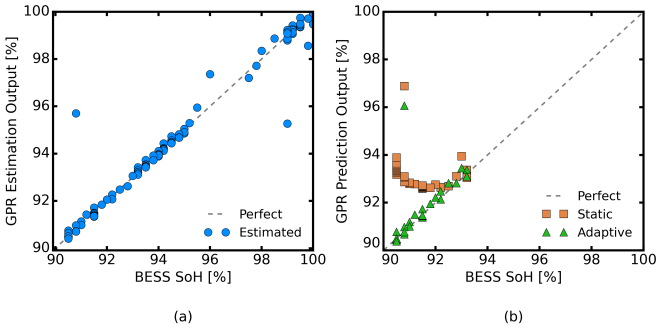

Fig. 7. Parity plots between the GPR method results and the reported BESS operational SoH data. The SoH (a) estimation and (b) static and adaptive prediction methods, with the estimation and adaptive results closely following the parity line.

Table II
GPR Performance Metrics for SoH Estimation and Prediction.

				Excl. Outlier*	
Metric	Estimation	Static	Adaptive	Static	Adaptive
MAE (%)	0.192	1.962	0.262	1.841	0.120
RMSE (%)	0.640	2.407	0.931	2.189	0.163
R^2	0.968	-4.793	0.131	-3.721	0.973
Bias (SoH pts)	0.012	1.765	0.163	1.654	0.032
95% CI Coverage (%)	90.0	47.5	90.0	48.7	89.7

* Excludes the September 23rd, 2021 prediction following the large offline period shown in Fig. 6.

The parity plots in Fig. 7 compare the results of the algorithm's three methods with the reported operational BESS SoH data. The estimation and adaptive prediction method results for the BMS reported data show strong alignment with the BESS dataset. Performance metrics are included in Table II with metrics mean absolute error (MAE), root mean square error (RMSE), coefficient of determination (R^2), bias, and 95% confidence interval (CI) coverage. The estimation method performs well, including 0.968 R^2, 0.192 percent MAE, and 0.640 percent RMSE. The adaptive method results contain a large outlier due to a large offline period which does not have any updates to SoH. In future studies, the estimation could support filling this gap with example experimental offline SoH data. Considering all other points, the adaptive method greatly improves over the static prediction case with metric results 0.973 R^2, 0.120 percent MAE, and 0.163 percent RMSE.

V. Conclusion

This study analyzes an example large-scale 1MW/2MWh field pilot operational BESS dataset to determine the priority input features and cycling data points to adaptively predict battery aging during operational charging conditions over long-term data. The developed algorithm expands the use of GPR for application to large-scale BESS datasets and is utilized for three methods: SoH estimation using shuffled five fold cross validation, static prediction as a base prediction case, and adaptive prediction with continuous refitting. In a proposed method based on cycling analysis, training events for the GPR model are extracted from the example dataset to selectively train the algorithm during windows with high percent capacity utilization to improve model accuracy.

Trained on BMS reported SoH data and high-resolution input features, the algorithm showed strong alignment with the BESS operational SoH data for both SoH estimation and adaptive refitting. The GPR estimation method yields a percent MAE of 0.192 and RMSE of 0.640 with the example BESS dataset and may be applied in future studies to fill historical gaps in SoH datasets. The GPR adaptive prediction refitting method was successfully employed, continuously refitting as it included new data points to adjust for changes in the operational dataset over the course of a year for projecting future SoH values. Excluding the post extended outage outlier, this method performs substantially better than the static prediction base case, adapting to the nonlinear changes in aging, with percent MAE and RMSE of 0.120 and 0.163.

Acknowledgment

Grant Fischer's Ph.D. studies are supported by a SMART Scholarship funded by OUSW/R&E, National Defense Education Program (NDEP) / BA-1, Basic Research. The support of the University of Kentucky the L. Stanley Pigman Chair in Power endowment is also gratefully acknowledged. Special thanks are due to industrial and academic mentors Aron Patrick, Rosemary Alden, and Kwabena Kyeremeh for their invaluable technical advice. Any opinions, findings, and conclusions or recommendations expressed in this material are those of the authors and do not necessarily reflect the views of sponsoring organizations.

References

[1] K. R. Ngoy *et al.*, "Lithium-ion batteries and the future of sustainable energy: A comprehensive review," *Renewable and Sustainable Energy Reviews*, vol. 223, p. 115971, 2025. [Online]. Available: https://www.sciencedirect.com/science/article/pii/S1364032125006446

[2] Y. Preger, R. Wittman, S. J. Harris, and M. Dubarry, "Are capacity and energy loss equivalent metrics for battery aging reporting?" *Journal of Electrochemical Energy Conversion and Storage*, vol. 23, no. 2, p. 021109, 03 2026. [Online]. Available: https://doi.org/10.1115/1.4071224

[3] P. M. Attia *et al.*, "Review—"knees" in lithium-ion battery aging trajectories," *Journal of The Electrochemical Society*, vol. 169, no. 6, p. 060517, 2022. [Online]. Available: http://dx.doi.org/10.1149/1945-7111/ac6d13

[4] X. Li *et al.*, "A perspective: Accelerating electrochemical energy storage for a reliable, affordable, resilient, and secure electric grid," *Batteries & Supercaps*, vol. 9, no. 3, p. e202500746, 2026.

[5] H. Rauf, M. S. Gul, M. Khalid, and N. Arshad, "Smart feature selection-based machine learning framework for calendar loss prediction of li-ion electric vehicle battery," in *2023 12th International Conference on Renewable Energy Research and Applications (ICRERA)*, 2023, pp. 300–303.

[6] T. F. Scholz, F. Pautzke, and B. Schmuelling, "In-situ determination of battery state of health considering the remaining capacity in electric vehicles - a case study," in *2025 14th International Conference on Renewable Energy Research and Applications (ICRERA)*, 2025, pp. 705–710.

[7] J. Schaeffer, E. Lenz, D. Gulla, M. Z. Bazant, R. D. Braatz, and R. Findeisen, "Gaussian process-based online health monitoring and fault analysis of lithium-ion battery systems from field data," *Cell Reports Physical Science*, vol. 5, no. 11, p. 102258, 2024. [Online]. Available: https://www.sciencedirect.com/science/article/pii/S2666386424005630

[8] K. A. Kyeremeh, S. E. Lavin, G. M. Fischer, D. M. Ionel, and A. Patrick, "Utility-scale battery energy storage systems—field pilot unit experience, analysis, and review of technological advancements," *IEEE Access*, vol. 14, pp. 74 274–74 288, 2026.

[9] "BESS-Analysis: Dataset for utility-scale battery energy storage systems—field pilot unit experience, analysis, and review of technological advancements," 2026. [Online]. Available: https://github.com/PPLResearch/BESS-Analysis

[10] O. Akeyo, V. Rallabandi, N. Jewell, A. Patrick, and D. Ionel, "Parameter identification for cells, modules, racks, and battery for utility-scale energy storage systems," *IEEE Access*, vol. 8, pp. 215 817–215 826, 01 2020.

[11] J. A. Braun, R. Behmann, D. Schmider, and W. G. Bessler, "State of charge and state of health diagnosis of batteries with voltage-controlled models," *Journal of Power Sources*, vol. 544, p. 231828, 2022. [Online]. Available: https://www.sciencedirect.com/science/article/pii/S0378775322008175

[12] M. Berecibar, I. Gandiaga, I. Villarreal, N. Omar, J. Van Mierlo, and P. Van den Bossche, "Critical review of state of health estimation methods of li-ion batteries for real applications," *Renewable and Sustainable Energy Reviews*, vol. 56, pp. 572–587, 2016. [Online]. Available: https://www.sciencedirect.com/science/article/pii/S1364032115013076

[13] R. Martins, H. C. Hesse, J. Jungbauer, T. Vorbuchner, and P. Musilek, "Optimal component sizing for peak shaving in battery energy storage system for industrial applications," *Energies*, vol. 11, no. 8, p. 2048, Aug. 2018.

[14] V. N. Lam, X. Cui, F. Stroebl, M. Uppaluri, S. Onori, and W. C. Chueh, "A decade of insights: Delving into calendar aging trends and implications," *Joule*, vol. 9, no. 1, p. 101796, 2025. [Online]. Available: https://www.sciencedirect.com/science/article/pii/S2542435124005105

[15] ——, "Calendar aging dataset for commercial lithium-ion cells," Open Science Framework, 2025. [Online]. Available: https://osf.io/ju325/

[16] K. Maher and N. Yerken, "Thermal degradation and safety assessment of li-ion battery cells in harsh climates," in *2025 14th International Conference on Renewable Energy Research and Applications (ICRERA)*, 2025, pp. 371–375.

[17] X. Li, D. Yu, S. B. Vilsen, V. R. Subramanian, and D.-I. Stroe, "Robust Remaining Useful Lifetime Prediction for Lithium-Ion Batteries With Dual Gaussian Process Regression-Based Ensemble Strategies on Limited Sample Data," *IEEE Transactions on Transportation Electrification*, vol. 11, no. 2, pp. 6279–6290, Jan. 2025.